

Structure Preserving Model Order Reduction by Parameter Optimization*

Paul Schwerdtner[†] and Matthias Voigt[‡]

December 22, 2024

Abstract

Model order reduction (MOR) methods that are designed to preserve structural features of a given full order model (FOM) often suffer from a lower accuracy when compared to their non structure preserving counterparts. In this paper, we present a framework for MOR based on direct parameter optimization. This means that the elements of the system matrices are iteratively varied to minimize an objective functional that measures the difference between the FOM and the reduced order model (ROM). Structural constraints are encoded in the parametrization of the ROM. The method only depends on frequency response data and can thus be applied to a wide range of dynamical systems.

We illustrate the effectiveness of our method on a port-Hamiltonian and on a symmetric second order system in a comparison with other structure preserving MOR algorithms.

1 Introduction

The increased demand for analysis and control of interconnected systems has promoted the investigation of structured models that encode physical properties of the underlying system such as stability or passivity. This is useful as these properties are hard to check or enforce for system interconnections but are often automatically given in structured models. When (sub)-systems describe complex physical phenomena, high-fidelity modeling often leads to models with a large state-space dimension which renders simulations or controller synthesis computationally challenging or even impossible.

This problem is addressed by model order reduction (MOR). MOR allows to compute low order surrogate models that approximate the original model's input/output map, i. e., the same excitation of the full order model (FOM) and the reduced order model (ROM) leads to a similar response and the ROM can be used in simulations or for controller design instead of the FOM. In the setting of interconnected systems, it is essential to not only mimic the given input/output map of some component but also preserve its physical structure to be able to still benefit from the automatic properties of structured models.

*This work is supported by the German Research Foundation (DFG) within the project VO2243/2-1: “Interpolationsbasierte numerische Algorithmen in der robusten Regelung” and the DFG Cluster of Excellence MATH+ within the project AA4-5: “Energy-based modeling, simulation, and optimization of power systems under uncertainty”.

[†]Corresponding author, Technische Universität Berlin, Institut für Mathematik, Straße des 17. Juni 136, 10623 Berlin, Germany. E-Mail: schwerdt@math.tu-berlin.de.

[‡]Universität Hamburg, Department of Mathematics, Bundesstraße 55, 20146 Hamburg, Germany, E-Mail: matthias.voigt@uni-hamburg.de; Technische Universität Berlin, Institut für Mathematik, Straße des 17. Juni 136, 10623 Berlin, Germany. E-Mail: mvoigt@math.tu-berlin.de.

For that, structure preserving MOR methods have been introduced. Throughout this paper, we consider the MOR of port-Hamiltonian (pH) systems (see [46] for an overview) of the form

$$\Sigma_{\text{pH}} : \begin{cases} \dot{x}(t) = (J - R)Qx(t) + Bu(t), \\ y(t) = B^T Qx(t), \end{cases}$$

where $J, R, Q \in \mathbb{R}^{n_x \times n_x}$ and $B \in \mathbb{R}^{n_x \times n_u}$ with the structural constraints $J = -J^T$, $R \geq 0$, and $Q \geq 0$. Note that often $Q > 0$ is assumed, e.g., in [6], but for simplicity of presentation we assume that $Q \geq 0$. The *Hamiltonian* $H : \mathbb{R}^n \rightarrow \mathbb{R}^+ := \{a \in \mathbb{R} \mid a \geq 0\}$ of Σ_{pH} is given by

$$H(x(t)) = \frac{1}{2}x(t)^T Qx(t).$$

It describes the total internal energy of the system in the state $x(t)$.

The other system class we consider consists of symmetric second order systems (SSO) with co-located force actuators and position sensors which usually arise in the modeling of mechanical systems. They are of the form

$$\Sigma_{\text{sso}} : \begin{cases} M\ddot{x}(t) + D\dot{x}(t) + Kx(t) = Bu(t), \\ y(t) = B^T x(t), \end{cases}$$

where $M, D, K \in \mathbb{R}^{n_x \times n_x}$ and $B \in \mathbb{R}^{n_x \times n_u}$ and where $M \geq 0$, $D \geq 0$, and $K \geq 0$. Such systems are discussed, e.g., in [33, 36]. In a similar fashion, we could consider systems with co-located velocity instead of position outputs. The latter can be shown to be pH by an appropriate transformation to first-order form.

Our goal is to compute ROMs which share exactly the same structural features as the FOMs. For a pH system this means that we want to obtain a ROM of the form

$$\Sigma_{\text{pH},r} : \begin{cases} \dot{x}_r(t) = (J_r - R_r)Q_r x_r(t) + B_r u(t), \\ y_r(t) = B_r^T Q_r x_r(t), \end{cases}$$

where $J_r, R_r, Q_r \in \mathbb{R}^{r \times r}$, $B_r \in \mathbb{R}^{r \times n_u}$ with $J_r = -J_r^T$, $R_r \geq 0$, and $Q_r \geq 0$ and with $r \ll n_x$. Analogously, a ROM for the system Σ_{sso} would be of the form

$$\Sigma_{\text{sso},r} : \begin{cases} M_r \ddot{x}_r(t) + D_r \dot{x}_r(t) + K_r x_r(t) = B_r u(t), \\ y_r(t) = B_r^T x_r(t), \end{cases} \quad (1)$$

where $M_r, D_r, K_r \in \mathbb{R}^{r \times r}$ and $B \in \mathbb{R}^{r \times n_u}$ with $M_r \geq 0$, $D_r \geq 0$, $K_r \geq 0$, and $r \ll n_x$.

In the literature there exist several different approaches to MOR and multiple different algorithms have been developed. Popular classes of reduction algorithms for linear time-invariant systems are the following: (i) eigenvalue based approaches such as *modal truncation* in which dominant eigenvalues of an underlying eigenvalue problem are extracted; (ii) balancing based methods such as *balanced truncation (BT)* in which input and output energies are considered to identify states which contribute only little to the input/output behavior of the system; and (iii) rational approximation methods such as *moment matching* or the *iterative rational Krylov algorithm (IRKA)* in which approximation techniques for the system's transfer function are employed. We refer to the textbooks [2] and [3] for an overview.

Structure preserving variants of the above mentioned methods have been considered intensively in the literature. For example, the works [20, 24, 34, 35, 49] treat the case of pH systems, while

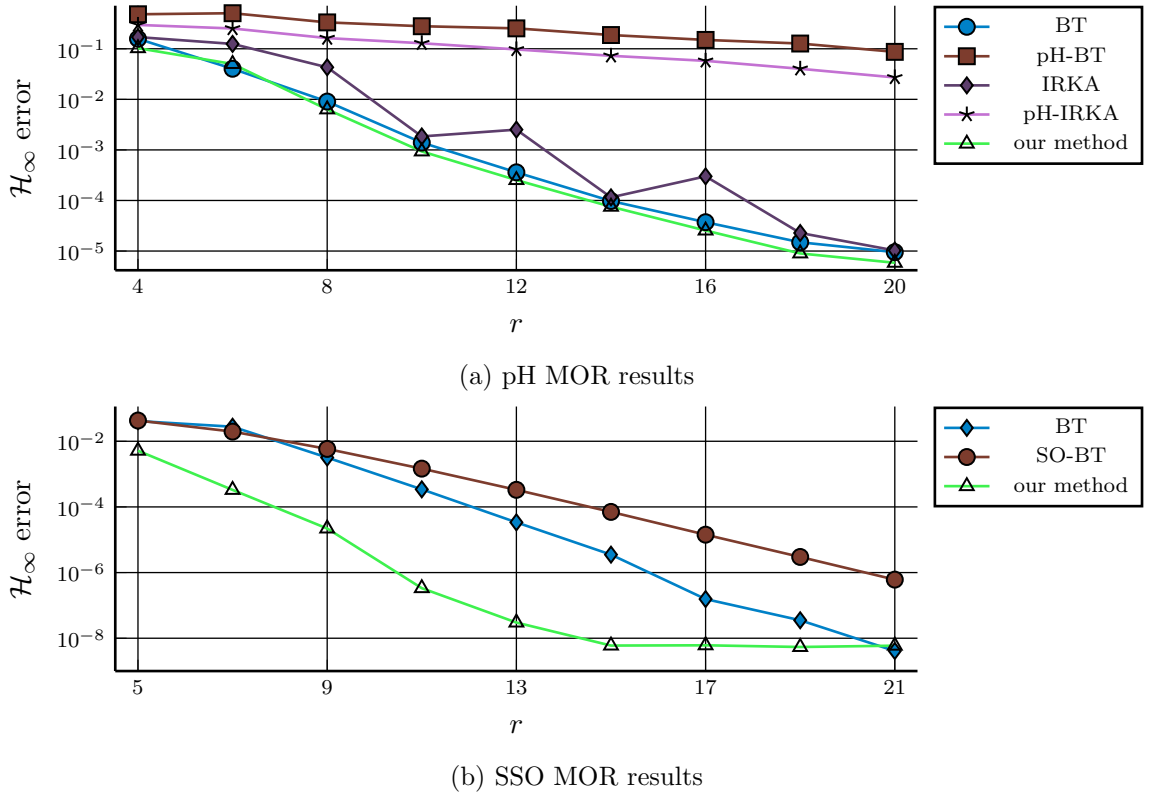


Figure 1: Comparison of the \mathcal{H}_∞ error of structure preserving MOR methods with non structure preserving MOR methods for varying reduced order models' state dimension r . Note that we have used a first-order representation of the second-order model to compute the BT ROMs in (b).

[4, 8, 13, 17, 23, 29, 32, 36, 37, 39–41] consider the case of second-order systems. Furthermore, recent advances in the backward error analysis of the structured eigenvalue problems associated with the system classes under consideration [16, 27] are of potential use in the derivation of eigenvalue based reduction methods for pH and SSO systems. Note that port-Hamiltonian systems are also *passive*. In rough terms, this means that such systems cannot internally produce energy. The preservation of this property is also addressed in many articles such as [22, 25, 31, 44], just to mention a few.

All the methods mentioned above have in common that they are projection-based methods, i.e., the involved matrices are reduced by an appropriate multiplication with long and skinny projection matrices. In contrast to that we develop a new framework which is based on making an ansatz for the structure of the ROM and then optimizing the entries of the resulting ROM parametrization. For the optimization we introduce a least squares type objective functional which measures the differences between the transfer functions of the FOM and the ROM.

The motivation for developing our new approach is the observation that for the same reduced order, the structure preserving variants of the balancing and interpolatory MOR methods often lead to a lower accuracy of the input/output map than their non structure preserving counterparts. This is illustrated in Figure 1, in which we display the \mathcal{H}_∞ error for different ROMs with varying reduced state space dimension including our new approach. The underlying models and MOR algorithms

are explained in the following section. Here we want to emphasize the much lower accuracy of the structure preserving methods of several orders of magnitude compared to the non structure preserving ones. On the other hand, our direct optimization approach allows to compute ROMs with a prescribed model structure that have an \mathcal{H}_∞ (and also \mathcal{H}_2) error that is closer to the respective error of ROMs created with non structure preserving MOR.

Our paper is organized as follows. In the next section, we discuss a few basics of MOR and briefly explain the structure preserving methods that we use for a comparison with our approach. After that, in Section 3, we derive our method. In particular, we discuss parametrizations of the system structures under consideration and the gradients of the error transfer functions between the FOM and the ROM with respect to the ROM parameters in Theorems 3.1 and 3.2. This enables us to use gradient based optimization to reduce this error and to achieve a close matching between the FOM and the ROM. Certain implementation variants are introduced in Section 4 while in Section 5 we test our algorithm on a couple of benchmark systems. There we will also see the superior approximation quality compared to the methods existing in the literature.

2 Background

In this section we give a few details on the most popular methods for MOR of linear time-invariant systems. We also briefly outline how these methods can be adapted to preserve model structures. In particular, we give some details on the methods we use for benchmarking our approach.

2.1 Model Order Reduction Overview

In the general linear MOR framework we consider a FOM of the form

$$\Sigma : \begin{cases} \dot{x}(t) = Ax(t) + Bu(t), \\ y(t) = Cx(t) + Du(t), \end{cases}$$

where $A \in \mathbb{R}^{n_x \times n_x}$, $B \in \mathbb{R}^{n_x \times n_u}$, $C \in \mathbb{R}^{n_y \times n_x}$, and $D \in \mathbb{R}^{n_y \times n_y}$. The goal of MOR is finding a ROM

$$\Sigma_r : \begin{cases} \dot{x}_r(t) = A_r x_r(t) + B_r u(t), \\ y_r(t) = C_r x_r(t) + D_r u(t), \end{cases}$$

where $A \in \mathbb{R}^{r \times r}$, $B \in \mathbb{R}^{r \times n_u}$, $C \in \mathbb{R}^{n_y \times r}$, and $D \in \mathbb{R}^{n_y \times n_y}$ and $r \ll n_x$. Moreover, $\|y - y_r\|$ should be small for all admissible inputs $u(\cdot)$ in an appropriate norm and if Σ is asymptotically stable (equivalently, all eigenvalues of A have negative real part), one typically requests that also Σ_r is asymptotically stable [2].

To measure the reduction error one usually considers the transfer functions

$$G(s) := C(sI_{n_x} - A)^{-1}B + D, \quad G_r(s) = C_r(sI_r - A_r)^{-1}B_r + D_r.$$

If Σ and Σ_r are asymptotically stable, then G and G_r are elements of the *Hardy spaces*

$$\begin{aligned} \mathcal{H}_2^{n_y \times n_u} &:= \left\{ H : \mathbb{C}^+ \rightarrow \mathbb{C}^{n_y \times n_u} \mid H \text{ is analytic and } \sup_{\sigma > 0} \int_{-\infty}^{\infty} \|H(\sigma + i\omega)\|_{\text{F}}^2 d\omega < \infty \right\}, \\ \mathcal{H}_\infty^{n_y \times n_u} &:= \left\{ H : \mathbb{C}^+ \rightarrow \mathbb{C}^{n_y \times n_u} \mid H \text{ is analytic and } \sup_{\lambda \in \mathbb{C}^+} \|H(\lambda)\|_2 < \infty \right\}, \end{aligned}$$

where $\mathbb{C}^+ := \{\lambda \in \mathbb{C} \mid \operatorname{Re}(\lambda) > 0\}$. Since in our setting, both G and G_r are real-rational functions, we also make use of the real-rational subspaces of $\mathcal{H}_2^{n_y \times n_u}$ and $\mathcal{H}_\infty^{n_y \times n_u}$ which we denote by $\mathcal{RH}_2^{n_y \times n_u}$ and $\mathcal{RH}_\infty^{n_y \times n_u}$, respectively. Since any function $G \in \mathcal{H}_2^{n_y \times n_u}$ or $G \in \mathcal{H}_\infty^{n_y \times n_u}$ is analytic in \mathbb{C}^+ , it can be uniquely analytically extended to the imaginary axis and thus, $G(i\omega)$ is well-defined for all $\omega \in \mathbb{R}$. The spaces $\mathcal{H}_2^{n_y \times n_u}$ and $\mathcal{H}_\infty^{n_y \times n_u}$ are Banach spaces ($\mathcal{H}_2^{n_y \times n_u}$ is even a Hilbert space) and are equipped with the norms

$$\|G\|_{\mathcal{H}_2} := \left(\frac{1}{2\pi} \int_{-\infty}^{\infty} \|G(i\omega)\|_F^2 d\omega \right)^{1/2}, \quad \|G\|_{\mathcal{H}_\infty} := \sup_{\omega \in \mathbb{R}} \|G(i\omega)\|_2. \quad (2)$$

With these concepts at hand, the error of the reduction procedure can be quantified by $\|G - G_r\|_{\mathcal{H}_2}$ or $\|G - G_r\|_{\mathcal{H}_\infty}$ and can either be optimized or bounded by the reduction algorithms.

We briefly mention the ideas of some of the most popular reduction algorithms, namely *balanced truncation (BT)* and the *iterative rational Krylov algorithm (IRKA)*, see the textbooks [2, 3]. Note that both methods assume that the FOM is asymptotically stable. BT is based on energy functionals related to the system. For some state $x_0 \in \mathbb{R}^{n_x}$ these functionals measure the input energy needed to steer the state from zero to x_0 (when this is possible) and the energy that can be extracted from the output, if the initial state is x_0 . Both energy functionals are quadratic forms of x_0 which are described by the symmetric and positive semidefinite controllability and observability Gramians $\mathcal{P}, \mathcal{Q} \in \mathbb{R}^{n_x \times n_x}$. In BT one computes a balancing transformation by an invertible matrix $T \in \mathbb{R}^{n_x \times n_x}$ such that the transformed Gramians are diagonal and equal, i. e.,

$$T^{-1}\mathcal{P}T^{-\top} = T^\top\mathcal{Q}T = \operatorname{diag}(\sigma_1, \dots, \sigma_n), \quad \sigma_1 \geq \sigma_2 \geq \dots \geq \sigma_n \geq 0.$$

The matrix T can be obtained from the Gramians \mathcal{P} and \mathcal{Q} whose computation or approximation is the most expensive part of the method. More precisely, \mathcal{P} and \mathcal{Q} are the unique solutions of the *Lyapunov equations*

$$A\mathcal{P} + \mathcal{P}A^\top + BB^\top = 0, \quad A^\top\mathcal{Q} + \mathcal{Q}A + C^\top C = 0.$$

If the system is controllable and observable, then $\mathcal{P} > 0$ and $\mathcal{Q} > 0$. Then with the Cholesky factorizations $\mathcal{P} = \mathcal{R}\mathcal{R}^\top$ and $\mathcal{Q} = \mathcal{L}\mathcal{L}^\top$ and the singular value decomposition $\mathcal{L}^\top\mathcal{R} = U\Sigma V^\top$ we obtain the transformation matrix $T = \mathcal{R}V\Sigma^{-\frac{1}{2}}$ (with $T^{-1} = \Sigma^{-\frac{1}{2}}U^\top\mathcal{L}^\top =: W^\top$). Partitioning $T = [T_r, \tilde{T}]$ and $W^\top = [W_r, \tilde{W}]^\top$, where $T_r, W_r \in \mathbb{R}^{n_x \times r}$ we finally obtain the ROM by $A_r = W_r^\top A T_r$, $B_r = W_r^\top B$, $C_r = C T_r$, and $D_r = D$. If $\sigma_r > \sigma_{r+1}$, then the ROM constructed in this way is asymptotically stable and

$$\|G - G_r\|_{\mathcal{H}_\infty} \leq 2 \sum_{j=r+1}^{n_x} \sigma_j.$$

On the other hand, IRKA is based on interpolating the transfer function of the FOM and optimizing the interpolation points such that a locally \mathcal{H}_2 optimal ROM is obtained. The ROM is again obtained by projection, i. e., the ROM is given by $A_r = W_r^\top A T_r$, $B_r = W_r^\top B$, $C_r = C T_r$, and $D_r = D$ for some appropriately chosen projection matrices $T_r, W_r \in \mathbb{R}^{n_x \times r}$ with $W_r^\top T_r = I_r$. The algorithm makes use of the following fact: If $\{s_1, \dots, s_r\} \subset \mathbb{C}$ are chosen such that $s_i I_{n_x} - A$ are invertible for $i = 1, \dots, r$ and $\{b_1, \dots, b_r\} \subset \mathbb{C}^{n_u}$ and $\{c_1, \dots, c_r\} \subset \mathbb{C}^{n_y}$ are given right and left *tangential directions*, then

$$(s_i I_{n_x} - A)^{-1} B b_i \in \operatorname{im}(T_r), \quad (c_i^\top C (s_i I_{n_x} - A)^{-1})^\top \in \operatorname{im}(W_r)$$

implies that

$$G(s_i)b_i = G_r(s_i)b_i, \quad c_i^H G(s_i) = c_i^H G_r(s_i), \quad c_i^H G'(s_i)b_i = c_i^H G'_r(s_i)b_i. \quad (3)$$

It has been shown in [11, 19, 47] that interpolation points and tangential directions that lead to \mathcal{H}_2 optimal ROMs satisfy the first-order necessary optimality conditions

$$G(-\lambda_i)\hat{b}_i = G_r(-\lambda_i)\hat{b}_i, \quad \hat{c}_i^H G(-\lambda_i) = \hat{c}_i^H G_r(-\lambda_i), \quad \hat{c}_i^H G'(-\lambda_i)\hat{b}_i = \hat{c}_i^H G'_r(-\lambda_i)\hat{b}_i, \quad i = 1, \dots, r. \quad (4)$$

Therein, $\{\lambda_1, \dots, \lambda_r\}$ are the eigenvalues of A_r and $\hat{c}_i := C_r x_i$ and $\hat{b}_i := B_r^T y_i$, where $\{x_1, \dots, x_r\}$ and $\{y_1, \dots, y_r\}$ are the corresponding right and left eigenvectors with $y_i^H x_i = 1$ for $i = 1, \dots, r$. Since the poles and residues of this optimal ROM are not known a priori, IRKA sets up a fixed point iteration in order to converge to these optimal points by alternately updating the ROM and computing new interpolation points and tangential directions from this ROM. For the details, we refer to [19].

2.2 Structure Preserving Model Order Reduction Methods

In this section we briefly describe some extensions of BT and IRKA to the system structures that are considered in this paper. In particular, these are the methods that we use for comparison with our new approach in Section 5. We remark that, besides often worse approximation quality, the structure-preserving methods often lack desirable theoretical properties such as the existence of an error bound.

BT is adapted in [34] in several ways to preserve the pH structure. One method that is presented there is called *effort constraint balanced truncation (pH-BT)*. In pH-BT, the balancing transformation T from standard BT is applied to the system Σ_{pH} to construct the balanced pH system as

$$\Sigma_{\text{pH,bal}} : \begin{cases} \dot{x}_b(t) = (J_b - R_b)Q_b x_b(t) + B_b u(t), \\ y_b(t) = B_b^T Q_b x_b(t), \end{cases}$$

where $J_b := T^{-1}JT^{-\top}$, $R_b := T^{-1}RT^{-\top}$, $Q_b := T^T QT$, and $B_b = T^{-1}B$. Note that this transformation preserves the pH structure. By partitioning the transformed matrices as

$$J_b = \begin{bmatrix} J_{11} & J_{12} \\ J_{21} & J_{22} \end{bmatrix}, \quad R_b = \begin{bmatrix} R_{11} & R_{12} \\ R_{21} & R_{22} \end{bmatrix}, \quad Q_b = \begin{bmatrix} Q_{11} & Q_{12} \\ Q_{21} & Q_{22} \end{bmatrix}, \quad B_b = \begin{bmatrix} B_1 \\ B_2 \end{bmatrix}$$

with J_{11} , R_{11} , $Q_{11} \in \mathbb{R}^{r \times r}$, a pH ROM with state space dimension r is then defined by

$$\Sigma_{\text{pH,r}} : \begin{cases} \dot{x}_r(t) = (J_{11} - R_{11})(Q_{11} - Q_{12}Q_{22}^{-1}Q_{21})x_r(t) + B_1 u(t), \\ y_r(t) = B_1^T(Q_{11} - Q_{12}Q_{22}^{-1}Q_{21})x_r(t). \end{cases}$$

The adaption of IRKA to pH systems, called *pH-IRKA*, is studied in [20]. There the construction of a pH interpolant is achieved by using the following observation: If we construct the right projection matrix $T_r \in \mathbb{R}^{n_x \times r}$ such that for a set of interpolation points $\{s_1, \dots, s_r\} \subset \mathbb{C}$ (assumed to be closed under complex conjugation) and tangential directions $\{b_1, \dots, b_r\} \subset \mathbb{C}^{n_u}$ we have that

$$(s_i I_{n_x} - (J - R)Q)^{-1} B b_i \in \text{im}(T_r), \quad i = 1, \dots, r$$

and, moreover, choose the left projection matrix as $W_r := QT_r(T_r^\top QT_r)^{-1}$, then a pH ROM is given by

$$\Sigma_{\text{pH},r} : \begin{cases} \dot{x}_r(t) = (J_r - R_r)Q_r x_r(t) + B_r u(t), \\ y_r(t) = B_r^\top Q_r x_r(t), \end{cases}$$

where $J_r = W_r^\top JW_r$, $Q_r = T_r^\top QT_r$, $R_r = W_r^\top RW_r$, and $B_r = W_r^\top B$. This ROM does, in general, only fulfill the first of the tangential interpolation conditions in (3), but a fixed-point iteration in the flavor of standard IRKA can be set up to obtain a ROM that fulfills at least the first of the \mathcal{H}_2 optimality conditions in (4).

A modification of BT to SSO systems, called *second-order balanced truncation (SO-BT)*, is discussed in [36]. There, the original SSO system is rewritten as a symmetric first order system of the form

$$\Sigma_{\text{fo}} : \begin{cases} \begin{bmatrix} I_{n_x} & 0 \\ 0 & M \end{bmatrix} \dot{q}(t) = \begin{bmatrix} 0 & I_{n_x} \\ -K & -D \end{bmatrix} q(t) + \begin{bmatrix} 0 \\ B \end{bmatrix} u(t), \\ y(t) = \begin{bmatrix} B^\top & 0 \end{bmatrix} q(t). \end{cases}$$

Under the condition that K and M are invertible, the system above is a system of ordinary differential equations and if the system is asymptotically stable, we can apply standard BT to this system. The corresponding controllability and observability Gramians can be partitioned according to the block structure of the system, i. e.,

$$\mathcal{P} = \begin{bmatrix} \mathcal{P}_p & \mathcal{P}_{12} \\ \mathcal{P}_{12}^\top & \mathcal{P}_v \end{bmatrix}, \quad \mathcal{Q} = \begin{bmatrix} \mathcal{Q}_p & \mathcal{Q}_{12} \\ \mathcal{Q}_{12}^\top & \mathcal{Q}_v \end{bmatrix}.$$

In [36] it has been shown that in our case, $\mathcal{P}_p = \mathcal{Q}_v$. Moreover, if the system Σ_{fo} is controllable and observable, then there exists a Cholesky factorization $\mathcal{P}_p = \mathcal{R}_p \mathcal{R}_p^\top$ with an invertible matrix $\mathcal{R}_p \in \mathbb{R}^{n_x \times n_x}$ and we can compute the singular value decomposition $\mathcal{R}_p^\top M \mathcal{R}_p = U_p \Sigma U_p^\top$. Then with the transformation matrix $T := \mathcal{R}_p U_p \Sigma^{-\frac{1}{2}}$ we obtain the *position/velocity balanced system*

$$\Sigma_{\text{sso,bal}} : \begin{cases} T^\top M T \ddot{x}_b(t) + T^\top D T \dot{x}_b(t) + T^\top K T x_b(t) = T^\top B u(t), \\ y_b(t) = B^\top T x_b(t), \end{cases}$$

in which the correspondingly transformed position/velocity Gramians $\mathcal{P}_{p,\text{bal}}$ and $\mathcal{Q}_{v,\text{bal}}$ are diagonal and equal. By partitioning $T = [T_r, \tilde{T}]$, we finally obtain a SSO ROM as in (1) with the desired symmetries by setting $M_r = T_r^\top M T_r$, $K_r = T_r^\top K T_r$, $D_r = T_r^\top D T_r$, and $B_r = T_r^\top B$.

Note that an adaption of IRKA to second-order systems is still an open problem, but some advancements in the direction of optimality conditions are available in [5].

3 Our Method

Our method for computing low order pH or SSO realizations that approximate the input/output map of a given system is based on making an ansatz for a parametrized low order pH or SSO model, respectively, and then directly optimizing the model parameters. The objective functional that is minimized is based on the difference of the transfer functions of FOM and ROM evaluated on the imaginary axis.

Therefore, we first present a parametrization of pH and SSO systems. Then we discuss our proposed objective functional and explain our optimization procedure. This optimization is gradient based, so we further derive the gradients that are involved in this process.

3.1 Structured Parametrized Transfer Functions

Throughout the next sections, we will rely on the following functions to manage the construction of the system matrices from parameter vectors.

Definition 3.1 (Reshaping operations). *We define the following operations.*

a) *The function family*

$$\text{vtf}_m : \mathbb{C}^{n \cdot m} \rightarrow \mathbb{C}^{n \times m}, \quad v \mapsto \begin{bmatrix} v_1 & v_{n+1} & \dots & v_{m(n-1)+1} \\ v_2 & v_{n+2} & \dots & v_{m(n-1)+2} \\ \vdots & \vdots & & \vdots \\ v_n & v_{2n} & \dots & v_{nm} \end{bmatrix}$$

reshapes a vector into an accordingly sized matrix with m columns. Its inverse is given by

$$\text{ftv} : \mathbb{C}^{n \times m} \rightarrow \mathbb{C}^{n \cdot m}, \quad A \mapsto [a_{1,1} \ a_{1,2} \ \dots \ a_{n,1} \ a_{1,2} \ \dots \ a_{n,m}]^\top.$$

The latter is the standard vectorization operator which is commonly denoted by vec .

b) *The function*

$$\text{vtu} : \mathbb{C}^{n(n+1)/2} \rightarrow \mathbb{C}^{n \times n}, \quad v \mapsto \begin{bmatrix} v_1 & v_2 & \dots & v_n \\ 0 & v_{n+1} & \dots & v_{2n-1} \\ 0 & 0 & \ddots & \vdots \\ 0 & 0 & 0 & v_{n(n+1)/2} \end{bmatrix}$$

maps a vector of length $n(n+1)/2$ to an $n \times n$ upper triangular matrix, while the function

$$\text{utv} : \mathbb{C}^{n \times n} \rightarrow \mathbb{C}^{n(n+1)/2}, \quad A \mapsto [a_{1,1} \ a_{1,2} \ \dots \ a_{1,n} \ a_{2,2} \ \dots \ a_{n,n}]^\top$$

maps the upper triangular part of an $n \times n$ matrix to a vector.

c) *The function*

$$\text{vtsu} : \mathbb{C}^{n(n-1)/2} \rightarrow \mathbb{C}^{n \times n}, \quad v \mapsto \begin{bmatrix} 0 & v_1 & v_2 & \dots & v_{n-1} \\ 0 & 0 & v_n & \dots & v_{2n-2} \\ 0 & 0 & 0 & \ddots & \vdots \\ 0 & 0 & 0 & 0 & v_{n(n-1)/2} \\ 0 & 0 & 0 & 0 & 0 \end{bmatrix}$$

maps a vector of length $n(n-1)/2$ to an $n \times n$ strictly upper triangular matrix, while the function

$$\text{sutv} : \mathbb{C}^{n \times n} \rightarrow \mathbb{C}^{n(n-1)/2}, \quad A \mapsto [a_{1,2} \ a_{1,3} \ \dots \ a_{1,n} \ a_{2,3} \ \dots \ a_{n-1,n}]^\top$$

maps the strictly upper triangular part of an $n \times n$ matrix to a vector.

Using these reshaping operations, we can define a parametrization of pH and SSO systems as follows.

3.1.1 Parametrized Port-Hamiltonian Systems

We provide a parametrization of a pH system that automatically satisfies the given structural constraints on the system matrices. The following lemma is a direct consequence of this structure.

Lemma 3.1. *Let $\theta \in \mathbb{R}^{n_\theta}$ be a parameter vector with $n_\theta = n_x \left(\frac{3n_x+1}{2} + n_u \right)$. Furthermore, let θ be partitioned as $\theta := [\theta_J^\top, \theta_R^\top, \theta_Q^\top, \theta_B^\top]^\top$ with $\theta_J \in \mathbb{R}^{n_x(n_x-1)/2}$, $\theta_R, \theta_Q \in \mathbb{R}^{n_x(n_x+1)/2}$, and $\theta_B \in \mathbb{R}^{n_x \cdot n_u}$. Further define the matrices*

$$J(\theta) = \text{vtsu}(\theta_J)^\top - \text{vtsu}(\theta_J), \quad (5a)$$

$$R(\theta) = \text{vtu}(\theta_R)^\top \text{vtu}(\theta_R), \quad (5b)$$

$$Q(\theta) = \text{vtu}(\theta_Q)^\top \text{vtu}(\theta_Q), \quad (5c)$$

$$B(\theta) = \text{vtf}_{n_u}(\theta_B). \quad (5d)$$

Then, to each $\theta \in \mathbb{R}^{n_\theta}$ one can assign the pH system

$$\Sigma_{\text{pH}}(\theta) : \begin{cases} \dot{x}(t) = (J(\theta) - R(\theta)) Q(\theta) x(t) + B(\theta) u(t), \\ y(t) = B(\theta)^\top Q(\theta) x(t). \end{cases} \quad (6)$$

Conversely, to each pH system Σ_{pH} with n_x states and n_u inputs and outputs one can assign a vector $\theta \in \mathbb{R}^{n_\theta}$ such that $\Sigma_{\text{pH}} = \Sigma_{\text{pH}}(\theta)$ with $\Sigma_{\text{pH}}(\theta)$ as in (6).

In the next result, we provide the gradients of the norm of the difference between a given transfer function $G \in \mathcal{H}_\infty^{n_u \times n_u}$ (of a possibly large-scale system) and the transfer function of the pH system (6), given by

$$G_{\text{pH}}(s, \theta) = B(\theta)^\top Q(\theta) (sI_{n_x} - (J(\theta) - R(\theta)) Q(\theta))^{-1} B(\theta), \quad (7)$$

evaluated at some given value $s_0 \in \overline{\mathbb{C}^+} := \{\lambda \in \mathbb{C} \mid \text{Re}(\lambda) \geq 0\}$ with respect to the parameter vector θ .

Theorem 3.1. *Let $\theta_0 \in \mathbb{R}^{n_\theta}$ be given and assume that $G \in \mathcal{H}_\infty^{n_u \times n_u}$ and $G_{\text{pH}}(\cdot, \theta) \in \mathcal{RH}_\infty^{n_u \times n_u}$ as in (7). Suppose further that for given $s_0 \in \overline{\mathbb{C}^+}$, the maximum singular value of $G(s_0) - G_{\text{pH}}(s_0, \theta)$ is simple and let $\hat{u} \in \mathbb{C}^{n_u}$ and $\hat{v} \in \mathbb{C}^{n_u}$ be the corresponding left and right singular vectors, respectively.*

Then the function $\theta \mapsto \|G(s_0) - G_{\text{pH}}(s_0, \theta)\|_2$ is differentiable in a neighborhood of θ_0 . Moreover, we define the short-hand notations $J_0 := J(\theta_0)$, $R_0 := R(\theta_0)$, $Q_0 := Q(\theta_0)$, $B_0 := B(\theta_0)$ and suppose that

$$\mathcal{F}_0 := s_0 I_{n_x} - (J_0 - R_0) Q_0$$

is invertible. With

$$\begin{aligned} Y_1 &:= -Q_0 \mathcal{F}_0^{-1} B_0 \hat{v} \hat{u}^\top B_0^\top Q_0 \mathcal{F}_0^{-1}, \\ Y_2 &:= \mathcal{F}_0^{-1} B_0 \hat{v} (\hat{u}^\top B_0^\top + \hat{u}^\top B_0^\top Q_0 \mathcal{F}_0^{-1} (J_0 - R_0)), \end{aligned}$$

we obtain the gradient

$$\nabla_\theta \|G(s_0) - G_{\text{pH}}(s_0, \theta_0)\|_2 := [\text{d}\theta_J^\top, \text{d}\theta_R^\top, \text{d}\theta_Q^\top, \text{d}\theta_B^\top]^\top,$$

where

$$d\theta_J = \operatorname{Re}(\operatorname{sutv}(-Y_1 + Y_1^\top)), \quad (8a)$$

$$d\theta_R = \operatorname{Re}(\operatorname{utv}(\operatorname{vtu}(\theta_R)Y_1 + \operatorname{vtu}(\theta_R)Y_1^\top)), \quad (8b)$$

$$d\theta_Q = \operatorname{Re}(\operatorname{utv}(\operatorname{vtu}(\theta_Q)Y_2 + \operatorname{vtu}(\theta_Q)Y_2^\top)), \quad (8c)$$

$$d\theta_B = \operatorname{Re}(\operatorname{ftv}((\widehat{v}\widehat{u}^\top B_0^\top Q_0 \mathcal{F}_0^{-1})^\top + Q_0 \mathcal{F}_0^{-1} B_0 \widehat{v}\widehat{u}^\top)). \quad (8d)$$

Before we can prove Theorem 3.1, we need the following lemma concerning the reshaping functions.

Lemma 3.2. *Let $A \in \mathbb{C}^{m \times n}$ and let $e_i^{(j)} \in \mathbb{C}^j$ denote the i -th standard basis vector of \mathbb{C}^j . Then*

$$\operatorname{tr}\left(A \operatorname{vtf}_m(e_i^{(nm)})\right) = (e_i^{(nm)})^\top \operatorname{ftv}(A^\top). \quad (9)$$

Now let $m = n$ and define $n_1 := \frac{n(n+1)}{2}$ and $n_2 := \frac{n(n-1)}{2}$. Then

$$\operatorname{tr}\left(A \operatorname{vtu}(e_i^{(n_1)})\right) = (e_i^{(n_1)})^\top \operatorname{utv}(A^\top), \quad (10)$$

$$\operatorname{tr}\left(A \operatorname{vtsu}(e_i^{(n_2)})\right) = (e_i^{(n_2)})^\top \operatorname{sutv}(A^\top). \quad (11)$$

Proof. Note that $\operatorname{vtf}_m(e_i^{(nm)}) \in \mathbb{R}^{n \times m}$ can be expressed as $e_k^{(n)}(e_\ell^{(m)})^\top$, where $i = (\ell - 1)n + k$. Since the trace is invariant under cyclic permutations¹, we have

$$\operatorname{tr}\left(A \operatorname{vtu}(e_i^{(nm)})\right) = \operatorname{tr}\left(A e_k^{(n)}(e_\ell^{(m)})^\top\right) = \operatorname{tr}\left((e_\ell^{(m)})^\top A e_k^{(n)}\right) = a_{\ell,k}.$$

On the other hand, it can be verified from the definition of ftv that $(e_i^{(nm)})^\top \operatorname{ftv}(A^\top) = a_{\ell,k}$. The equalities (10) and (11) can be shown analogously by identifying the nonzero element of $\operatorname{vtu}(e_i^{(n_1)})$ and $\operatorname{vtsu}(e_i^{(n_2)})$, respectively, and using the cyclic permutation invariance of the trace. \square

We proceed with the proof of Theorem 3.1.

Proof. We show differentiability with respect to θ_J and accordingly the partial gradient (8a). Fix an $i \in \{1, \dots, n_x(n_x - 1)/2\}$ and let e_i be the i -th standard basis vector of $\mathbb{R}^{n_x(n_x - 1)/2}$. Let $d\theta_i(\varepsilon) := [\varepsilon e_i^\top, 0]^\top \in \mathbb{R}^{n_\theta}$ and $\Delta_i := J(e_i)$.

We have

$$\begin{aligned} G_{\text{pH}}(s_0, \theta_0 + d\theta_i(\varepsilon)) &= B_0^\top Q_0 (s_0 I_{n_x} - (J_0 + \varepsilon \Delta_i - R_0) Q_0)^{-1} B_0 \\ &= -B_0^\top Q_0 (\varepsilon \Delta_i Q_0 - \mathcal{F}_0)^{-1} B_0. \end{aligned}$$

Thus, $\varepsilon \mapsto G_{\text{pH}}(s_0, \theta_0 + d\theta_i(\varepsilon))$ is a rational matrix-valued function that admits a Taylor series expansion at zero which, according to [28], is

$$G_{\text{pH}}(s_0, \theta_0 + d\theta_i(\varepsilon)) = G_{\text{pH}}(s_0, \theta_0) + \varepsilon B_0^\top Q_0 \mathcal{F}_0^{-1} \Delta_i Q_0 \mathcal{F}_0^{-1} B_0 + \mathcal{O}(\varepsilon^2). \quad (12)$$

¹For arbitrary $X \in \mathbb{C}^{n \times m}$, $Y \in \mathbb{C}^{m \times p}$, and $Z \in \mathbb{C}^{p \times n}$ we have that $\operatorname{tr}(XYZ) = \operatorname{tr}(ZXY) = \operatorname{tr}(YZX)$.

Due to the simplicity assumption for the maximum singular value of $G(s_0) - G_{\text{pH}}(s_0, \theta_0)$, by [26] the function $\varepsilon \mapsto \|G(s_0) - G_{\text{pH}}(s_0, \theta_0 + d\theta_i(\varepsilon))\|_2$ is differentiable at zero. Together with (12) we obtain

$$\begin{aligned} \frac{d}{d\varepsilon} \|G(s_0) - G_{\text{pH}}(s_0, \theta_0 + d\theta_i(\varepsilon))\|_2 \Big|_{\varepsilon=0} &= -\text{Re}(\hat{u}^H B_0^T Q_0 \mathcal{F}_0^{-1} \Delta_i Q_0 \mathcal{F}_0^{-1} B_0 \hat{v}) \\ &= -\text{Re}(\text{tr}(Q_0 \mathcal{F}_0^{-1} B_0 \hat{v} \hat{u}^H B_0^T Q_0 \mathcal{F}_0^{-1} \Delta_i)) \\ &= \text{Re}(\text{tr}(Y_1 \Delta_i)). \end{aligned}$$

Since $\Delta_i = \text{vtsu}(e_i)^T - \text{vtsu}(e_i)$ we have

$$\begin{aligned} \text{Re}(\text{tr}(Y_1 \Delta_i)) &= \text{Re}(\text{tr}(Y_1(\text{vtsu}(e_i)^T - \text{vtsu}(e_i)))) \\ &= \text{Re}(\text{tr}(Y_1 \text{vtsu}(e_i)^T) - \text{tr}(Y_1 \text{vtsu}(e_i))) \\ &= \text{Re}(\text{tr}((Y_1^T - Y_1) \text{vtsu}(e_i))) = (d\theta_J)_i. \end{aligned}$$

The last equality is due to Lemma 3.2. Differentiability with respect to the other components of θ can be shown analogously as well as the formulas (8b)–(8d), again by making use of Lemma 3.2. \square

3.1.2 Parametrized Mechanical Systems

Similarly to the previous parametrization of pH systems, we can proceed in the case of SSO systems.

Lemma 3.3. *Let $\theta \in \mathbb{R}^{n_\theta}$ be a parameter vector with $n_\theta = n_x \left(\frac{3n_x+3}{2} + n_u \right)$. Furthermore, let θ be partitioned as $\theta := [\theta_M^T, \theta_D^T, \theta_K^T, \theta_B^T]^T$ with $\theta_M, \theta_D, \theta_K \in \mathbb{R}^{n_x(n_x+1)/2}$ and $\theta_B \in \mathbb{R}^{n_x \cdot n_u}$. Further define the matrices*

$$M(\theta) = \text{vtu}(\theta_M)^T \text{vtu}(\theta_M), \quad (13a)$$

$$D(\theta) = \text{vtu}(\theta_D)^T \text{vtu}(\theta_D), \quad (13b)$$

$$K(\theta) = \text{vtu}(\theta_K)^T \text{vtu}(\theta_K), \quad (13c)$$

$$B(\theta) = \text{vtf}_{n_u}(\theta_B). \quad (13d)$$

Then, to each $\theta \in \mathbb{R}^{n_\theta}$ one can assign the second order system

$$\Sigma_{\text{sso}}(\theta) : \begin{cases} M(\theta) \ddot{x}(t) + D(\theta) \dot{x}(t) + K(\theta) x(t) = B(\theta) u(t), \\ y(t) = B(\theta)^T x(t). \end{cases} \quad (14)$$

Conversely, to each SSO system Σ_{sso} with n_x states and n_u inputs and outputs one can assign a vector $\theta \in \mathbb{R}^{n_\theta}$ such that $\Sigma_{\text{sso}} = \Sigma_{\text{sso}}(\theta)$ with $\Sigma_{\text{sso}}(\theta)$ as in (14).

Next, we formulate the analogue of Theorem 3.1. Again we provide the gradients of the norm of the difference between a given transfer function $G \in \mathcal{H}_\infty^{n_u \times n_u}$ (of a possibly large-scale system) and the transfer function of the SSO system (14), given by

$$G_{\text{sso}}(s, \theta) = B(\theta)^T (s^2 M(\theta) + s D(\theta) + K(\theta))^{-1} B(\theta), \quad (15)$$

evaluated at some given value $s_0 \in \overline{\mathbb{C}^+}$ with respect to the parameter vector θ .

Theorem 3.2. *Let $\theta_0 \in \mathbb{R}^{n_\theta}$ be given and assume that $G \in \mathcal{H}_\infty^{n_u \times n_u}$ and $G_{\text{sso}}(\cdot, \theta) \in \mathcal{RH}_\infty^{n_u \times n_u}$ as in (15). Suppose further that for given $s_0 \in \overline{\mathbb{C}^+}$, the maximum singular value of $G(s_0) - G_{\text{sso}}(s_0, \theta)$ is simple and let $\hat{u} \in \mathbb{C}^{n_u}$ and $\hat{v} \in \mathbb{C}^{n_u}$ be the corresponding left and right singular vectors, respectively.*

Then the function $\theta \mapsto \|G(s_0) - G_{\text{sso}}(s_0, \theta)\|_2$ is differentiable in a neighborhood of θ_0 . Define the short-hand notations $M_0 := M(\theta_0)$, $D_0 := D(\theta_0)$, $K_0 := K(\theta_0)$, $B_0 := B(\theta_0)$, and assume further that

$$\mathcal{F}_0 = s_0^2 M_0 + s_0 D_0 + K_0$$

is invertible. Then with

$$Y := \mathcal{F}_0^{-1} B_0 \hat{v} \hat{u}^H B_0^T \mathcal{F}_0^{-1},$$

we obtain

$$\nabla_\theta \|G(s_0) - G_{\text{sso}}(s_0, \theta)\|_2 := [\mathrm{d}\theta_M^T, \mathrm{d}\theta_D^T, \mathrm{d}\theta_K^T, \mathrm{d}\theta_B^T]^T,$$

where

$$\mathrm{d}\theta_M = \mathrm{Re}(s_0^2 \cdot \mathrm{vtv}(\mathrm{vtu}(\theta_M)Y + \mathrm{vtu}(\theta_M)Y^T)), \quad (16a)$$

$$\mathrm{d}\theta_D = \mathrm{Re}(s_0 \cdot \mathrm{vtv}(\mathrm{vtu}(\theta_D)Y + \mathrm{vtu}(\theta_D)Y^T)), \quad (16b)$$

$$\mathrm{d}\theta_K = \mathrm{Re}(\mathrm{vtv}(\mathrm{vtu}(\theta_K)Y + \mathrm{vtu}(\theta_K)Y^T)), \quad (16c)$$

$$\mathrm{d}\theta_B = \mathrm{Re}(\mathrm{ftv}(\mathcal{F}_0^{-1} B_0 (\hat{v} \hat{u}^H + \hat{u} \hat{v}^H))). \quad (16d)$$

Proof. The proof is analogous to the proof of Theorem 3.1. We again show differentiability with respect to θ_M and the corresponding partial gradient (16a). Fix $i \in \{1, \dots, n_x(n_x + 1)/2\}$ and let $\mathrm{d}\theta_i(\varepsilon) := [\varepsilon e_i^T \ 0]^T \in \mathbb{R}^{n_\theta}$. Note that $\varepsilon \mapsto M(\theta_0 + \mathrm{d}\theta_i(\varepsilon))$ admits a Taylor series expansion at 0. It is given by

$$M(\theta_0 + \mathrm{d}\theta_i(\varepsilon)) = \mathrm{vtu}(\theta_0 + \mathrm{d}\theta_i(\varepsilon))^T \mathrm{vtu}(\theta_0 + \mathrm{d}\theta_i(\varepsilon)) = M_0 + \varepsilon \Delta_i + \mathcal{O}(\varepsilon^2),$$

where $\Delta_i = \mathrm{vtu}(\theta_M)^T \mathrm{vtu}(e_i) + \mathrm{vtu}(e_i)^T \mathrm{vtu}(\theta_M)$. Therefore, the Taylor series expansion of $\varepsilon \mapsto G_{\text{sso}}(s_0, \theta_0 + \mathrm{d}\theta_i(\varepsilon))$ at zero is given by

$$\begin{aligned} G_{\text{sso}}(s_0, \theta_0 + \mathrm{d}\theta_i(\varepsilon)) &= B_0^T (\varepsilon s_0^2 \Delta_i + \mathcal{F}_0 + \mathcal{O}(\varepsilon^2))^{-1} B_0 \\ &= G_{\text{sso}}(s_0, \theta_0) - \varepsilon s_0^2 B_0^T \mathcal{F}_0^{-1} \Delta_i \mathcal{F}_0^{-1} B_0 + \mathcal{O}(\varepsilon^2). \end{aligned} \quad (17)$$

For the derivative of $\varepsilon \mapsto \|G(s_0) - G_{\text{sso}}(s_0, \theta_0 + \mathrm{d}\theta_i(\varepsilon))\|_2$ at zero, from (17), we obtain

$$\begin{aligned} \frac{d}{d\varepsilon} \|G(s_0) - G_{\text{sso}}(s_0, \theta_0 + \mathrm{d}\theta_i(\varepsilon))\|_2 \Big|_{\varepsilon=0} &= \mathrm{Re}(s_0^2 \hat{u}^H B_0^T \mathcal{F}_0^{-1} \Delta_i \mathcal{F}_0^{-1} B_0 \hat{v}) \\ &= \mathrm{Re}(s_0^2 \mathrm{tr}(\mathcal{F}_0^{-1} B_0 \hat{v} \hat{u}^H B_0^T \mathcal{F}_0^{-1} \Delta_i)) \\ &= \mathrm{Re}(s_0^2 \mathrm{tr}(Y \Delta_i)). \end{aligned}$$

Since $\Delta_i = \mathrm{vtu}(\theta_M)^T \mathrm{vtu}(e_i) + \mathrm{vtu}(e_i)^T \mathrm{vtu}(\theta_M)$, we have that

$$\begin{aligned} \mathrm{Re}(s_0^2 \mathrm{tr}(Y \Delta_i)) &= \mathrm{Re}(s_0^2 \mathrm{tr}(Y \mathrm{vtu}(\theta_M)^T \mathrm{vtu}(e_i)) + \mathrm{tr}(Y \mathrm{vtu}(e_i)^T \mathrm{vtu}(\theta_M))) \\ &= \mathrm{Re}(s_0^2 (e_i^T \mathrm{vtv}(\mathrm{vtu}(\theta_M)Y^T) + e_i^T \mathrm{vtv}(\mathrm{vtu}(\theta_M)Y))) = (\mathrm{d}\theta_M)_i. \end{aligned}$$

The other parts of the gradient can be shown analogously. \square

3.2 Optimization of the ROM Parameters

In the following, we will explain how we optimize the parameters of the ROM to minimize the distance of its transfer function to the transfer function of a given model with respect to the \mathcal{H}_∞ norm. Throughout the following section, we denote the transfer function of a given (large-scale) model by G and some parametrized transfer function approximation by $G_r(\cdot, \theta)$. We assume that $G \in \mathcal{H}_\infty^{n_u \times n_u}$ and will construct a sequence $(\theta_i)_{i \in \mathbb{N}}$ such that $G_r(\cdot, \theta_i) \in \mathcal{RH}_\infty^{n_u \times n_u}$ for $i = 0, 1, 2, \dots$ with the goal to achieve smaller errors for increasing values of i . This sequence should converge to a value $\theta_{\text{opt}} \in \mathbb{R}^{n_\theta}$ leading to a small \mathcal{H}_∞ error.

We will first explain the problems associated with directly minimizing $\|G - G_r(\cdot, \theta)\|_{\mathcal{H}_\infty}$ and after that detail our approach.

3.2.1 Problems with the Direct Optimization Approach

Methods for computing the \mathcal{H}_∞ norm of rational transfer functions exist since the early 1990s [9, 10]. However, these are typically not used for computing the \mathcal{H}_∞ norm of $G - G_r(\cdot, \theta)$, since they require multiple solutions of eigenvalue problems of size around twice the state space dimension of this error transfer function which has a slightly larger state space dimension than the state space realization of Σ of G . Since in the MOR context, Σ is assumed to be large and sparse, this is computationally prohibitive.

Recent developments have led to faster \mathcal{H}_∞ norm computation methods for transfer functions of systems with a large state space dimension [1, 18, 21, 43, 48]. However, with these methods, typically only a local maximizer of $\omega \mapsto \|G(i\omega)\|_2$ for $\omega \in \mathbb{R}$ is computed. This problem is addressed in [42], in which a global certificate for the \mathcal{H}_∞ norm computation is established.

Using a combination of a fast \mathcal{H}_∞ norm computation method with this global certificate in principle allows the direct optimization of the parameters of $G_r(\cdot, \theta)$ to minimize its distance to a given G in the \mathcal{H}_∞ norm. However, the problem

$$\min_{\theta \in \mathbb{R}^{n_\theta}} \|G - G_r(\cdot, \theta)\|_{\mathcal{H}_\infty} \quad (18)$$

is a nonlinear, nonsmooth, and nonconvex optimization problem. There exist many methods that solve nonsmooth optimization problems, e.g., [12, 14, 15, 38]. However, they tend to converge only slowly and may get stuck at local optimizers far from the global optimum. On top of that, despite the previously mentioned developments for the \mathcal{H}_∞ norm computation of large scale systems, the repeated evaluation of (18) is still computationally expensive. In Section 5 we compare our method with the direct optimization approach, for which we use the method in [43] as \mathcal{H}_∞ norm computation engine together with the method in [14] for solving the nonsmooth optimization problem directly.

3.2.2 Leveled Least Squares

Instead of minimizing $\|G - G_r(\cdot, \theta)\|_{\mathcal{H}_\infty}$ directly, we propose to minimize an alternative objective functional. Let $\gamma > 0$ be a parameter and $S := \{s_1, \dots, s_k\} \subset i\mathbb{R}$ be a set of sample points. We propose to minimize

$$L(\gamma, G, G_r(\cdot, \theta), S) := \frac{1}{\gamma} \sum_{s_i \in S} \left((\|G(s_i) - G_r(s_i, \theta)\|_2 - \gamma)_+ \right)^2, \quad (19)$$

where

$$(\cdot)_+ : \mathbb{R} \rightarrow \overline{\mathbb{R}^+}, \quad x \mapsto \begin{cases} x & \text{if } x \geq 0, \\ 0 & \text{if } x < 0 \end{cases}$$

for decreasing values of $\gamma > 0$. In the following proposition, we summarize the characteristics of L that motivate its utilization in \mathcal{H}_∞ error minimization.

Proposition 3.1 (Properties of L). *Let $S = \{s_1, \dots, s_k\} \subset i\mathbb{R}$ and $\gamma > 0$ be fixed and let L be given as in (19). For $i = 1, \dots, k$ define*

$$f_i(\theta) := \|G(s_i) - G_r(s_i, \theta)\|_2$$

and $g(\theta) := L(\gamma, G, G_r(\cdot, \theta), S)$. Then the following statements are satisfied:

- i) We have that $L(\gamma, G, G_r(\cdot, \theta), S) = 0$ for all $\gamma > \|G - G_r(\cdot, \theta)\|_{\mathcal{H}_\infty}$.
- ii) If for each $i = 1, \dots, k$, $G(s_i) - G_r(s_i, \theta_0)$ has a simple maximum singular value or $f_i(\theta_0) < \gamma$, then $g(\cdot)$ is differentiable at θ_0 . Moreover, the partial derivatives of $g(\cdot)$ at θ_0 are given by

$$\frac{\partial}{\partial \theta_j} g(\theta_0) = \frac{2}{\gamma} \sum_{f_i(\theta_0) > \gamma} (f_i(\theta_0) - \gamma) \frac{\partial}{\partial \theta_j} f_i(\theta_0), \quad j = 1, \dots, n_\theta. \quad (20)$$

Proof. Assertion i) follows directly from the definition of L . It remains to show ii): Clearly, if $f_i(\theta_0) < \gamma$, then by continuity of $f_i(\cdot)$, $f_i(\theta) < \gamma$ for all θ in some neighborhood of θ_0 . Thus, $((f_i(\cdot) - \gamma)_+)^2$ is differentiable near θ_0 and the gradient is zero. Assume now that $f_i(\theta_0) \geq \gamma$. If even $f_i(\theta_0) > \gamma$, then $((f_i(\theta) - \gamma)_+)^2 = (f_i(\theta) - \gamma)^2$ for all θ in a neighborhood of θ_0 . Hence, $((f_i(\cdot) - \gamma)_+)^2$ is differentiable at θ_0 , if the maximum singular value of $G(s_i) - G_r(s_i, \theta_0)$ is simple. Then by the chain rule we get

$$\frac{\partial}{\partial \theta_j} ((f_i(\theta) - \gamma)_+)^2 \Big|_{\theta=\theta_0} = 2(f_i(\theta_0) - \gamma) \frac{\partial}{\partial \theta_j} f_i(\theta_0), \quad j = 1, \dots, n_\theta, \quad (21)$$

where $\frac{\partial}{\partial \theta_j} f_i(\theta_0)$ is obtained by Theorem 3.1 or 3.2. It remains to consider the case $f_i(\theta_0) = \gamma$. Choose an arbitrary direction $\hat{\theta} \in \mathbb{R}^{n_\theta} \setminus \{0\}$. Then we have

$$f_i(\theta_0 + \varepsilon \hat{\theta}) = f_i(\theta_0) + \varepsilon (\nabla f_i(\theta_0))^\top \hat{\theta} + \mathcal{O}(\varepsilon^2).$$

This gives rise to

$$\begin{aligned} \lim_{\varepsilon \rightarrow 0} \frac{1}{\varepsilon} \left(((f_i(\theta_0 + \varepsilon \hat{\theta}) - \gamma)_+)^2 - ((f_i(\theta_0) - \gamma)_+)^2 \right) &= \lim_{\varepsilon \rightarrow 0} \frac{1}{\varepsilon} \left((\varepsilon (\nabla f_i(\theta_0))^\top \hat{\theta})_+ \right)^2 \\ &= \lim_{\varepsilon \rightarrow 0} \varepsilon \left(((\nabla f_i(\theta_0))^\top \hat{\theta})_+ \right)^2 = 0. \end{aligned}$$

Since the latter is true for arbitrary directions $\hat{\theta} \neq 0$, $((f_i(\cdot) - \gamma)_+)^2$ is differentiable at θ_0 and the gradient is zero. Finally, together with (21), we obtain (20). \square

Property i) establishes a connection between L and the \mathcal{H}_∞ optimization problem, while ii) facilitates gradient based optimization. If there exists a $\theta_0 \in \mathbb{R}^{n_\theta}$ such that $\gamma > \|G - G_r(\cdot, \theta_0)\|_{\mathcal{H}_\infty}$, then $f_i(\theta) < \gamma$ for all $i = 1, \dots, k$ and θ in a neighborhood of θ_0 . Hence θ_0 is a differentiable minimizer of L (which means that L is differentiable at θ_0) for fixed sample point set S and level γ . Otherwise, the minimizer of L may be attained at a non-differentiable point $\theta_{\text{opt}} \in \mathbb{R}^{n_\theta}$, if there exists one $s_i \in S$ such that the maximum singular value of $G(s_i) - G_r(s_i, \theta_{\text{opt}})$ is non-simple and greater or equal to γ .

We now outline an algorithm that uses L to compute ROMs and reason why a respective optimization of L yields ROMs which tend to have a small \mathcal{H}_∞ error.

Our method consists of 3 main steps: *initialization*, γ -*selection*, and *optimization*. During initialization, an initial ROM of a user-selected structure is computed. The initial ROM may be obtained using the FOM and interpolatory MOR or may also be just a random model that meets the required structural constraints. In Section 4, we provide a comparison of different initialization strategies. After initialization, L is minimized for decreasing values of γ . For that, in the γ -selection step, γ is set to some strictly positive value and the optimization is started. In our `julia` implementation, in the optimization step, we use the nonlinear optimization engine `OPTIM` [30] configured with the Broyden-Fletcher-Goldfarb-Shanno (BFGS) method for approximating the inverse Hessian matrix.

After the optimization of L for a fixed γ , in the γ -selection step, the optimization can either be called again with an increased or decreased value of γ or the process can be stopped. As an example for a γ -selection step, in our numerical experiments, we provide a fixed sequence of strictly positive and strictly monotonically decreasing values for γ . We stop the process for the first value of γ at which after optimization the value of L is greater than zero. We discuss different γ -selection strategies in Section 4.

At first it seems contradictory to minimize the sum of squares of the error transfer function evaluated at a fixed set of points to minimize its \mathcal{H}_∞ norm. This is because the \mathcal{H}_∞ norm is usually attained at a single point or a few points at most. Furthermore, minimizing the sum of squares of the errors usually does not minimize the maximal error value. For that reason, L contains the parameter γ which functions as a cut-off and allows to tune the least-squares optimization to get a good \mathcal{H}_∞ approximation.

In particular, by introducing γ we do not directly minimize the \mathcal{H}_∞ error but instead construct an objective functional that attains its global minimum at zero, when the error at all considered points is below a given threshold. Furthermore, the level γ allows to distinguish samples that are still relevant for the optimization of L from samples that can be ignored at the current iteration. However, note that a zero value of the objective functional does not imply that the \mathcal{H}_∞ norm of the error is below γ .

This approach has several benefits over the direct \mathcal{H}_∞ minimization. The \mathcal{H}_∞ norm does not need to be computed at every iteration and the samples of the large-scale transfer function can be reused in subsequent iterations, such that only $G_r(\cdot, \theta)$ needs to be recomputed after the parameters have been updated.

The most important benefit, however, is that when using L instead of the \mathcal{H}_∞ norm we use more information of the transfer function when computing the gradient. Instead of focusing on minimizing the error of the transfer function where it is currently maximized, we consider a set of points where the error is above a certain threshold and can in this way obtain a better global behavior. This is illustrated in the numerical experiments in Section 5. In the next section, we discuss several implementation variants.

4 Implementation Variants

Our method consists of the three steps *initialization*, γ -*selection*, and *optimization*. Each of these can be changed independently. In this sense, we rather propose a template method for obtaining ROMs based on optimization of the ROM parameters. In the following, we briefly outline a few different options for the initialization and the γ -selection step. For the optimization we have only used BFGS as implemented in [30].

4.1 Initialization

The task of the initialization step is to provide an initial ROM. The only constraint is that this ROM must satisfy the structural constraints imposed on the final ROM by the user. If the FOM already has the desired structure, then any appropriate structure preserving MOR method (such as the ones described in Subsection 2.2) can be used to obtain an initial ROM. If the FOM is does not satisfy the structural constraints or only frequency data is available, then an alternative way that does not use the FOM's system matrices must be used. We have tested three different ways of initialization. The first one is based on a fast greedy structure preserving MOR method and the following two are a random initialization and a ROM that minimizes the least-squares error over all sample points.

The fast greedy structure preserving MOR has been presented in [7]. The main idea is to combine the method for \mathcal{H}_∞ norm computation from [1, 43] with interpolatory MOR, i.e. iteratively compute the \mathcal{H}_∞ norm of the difference between the FOM and the ROM and update the ROM such that it interpolates the FOM at the point on the imaginary axis, where the \mathcal{H}_∞ norm is attained. While this method is fast and widely applicable, it suffers from a high error. This is due to the fact that the ROM obtained from greedy interpolation is only very accurate at the interpolation points but does not uniformly approximate the FOM. In our numerical experiments shown in Section 5, we have used this as initialization technique.

The other two initialization methods are based on the generation of random matrices that satisfy the structural constraints. The construction of such matrices (symmetric, skew-symmetric, positive semi-definite) from general random matrices is straightforward. We initialize our method both directly with random systems but also introduce a preliminary least-squares approximation step, in which the function

$$\text{lsq}(G, G_r(\cdot, \theta), S) := \sum_{s_i \in S} \|G(s_i) - G_r(s_i, \theta)\|_2^2,$$

where again G and $G_r(\cdot, \theta)$ are transfer functions of the FOM and ROM, respectively, is minimized using BFGS. The set S contains all samples that are also used during the minimization of L after the initialization. In our numerical experiments, these other two initialization techniques have also been tested but they have yielded inferior results.

4.2 γ -Selection

Since our method consists of multiple minimizations of L for different values of γ to find a ROM with small \mathcal{H}_∞ error, a method for choosing γ must be provided. Furthermore, it is the duty of the γ -selection step to determine when our method has terminated. We present two different algorithms for deciding on termination or defining the next γ within L in the course of our method. We explicitly assume that the ROM transfer functions of all intermediate iterates are well-defined and elements of $\mathcal{RH}_\infty^{n_u \times n_u}$. Note that this has always been satisfied in our numerical experiments. The problematic cases are those, where some of the matrices of our parametrization are only positive semi-definite. For example, the transfer function of the reduced SSO system $\Sigma_{\text{sso},r}$ in (1) is not well-defined, if, e.g., all the matrices M_r , D_r , and K_r are singular and have a common nonzero vector in their kernels. However, this problem can be solved by adding small multiples of the identity matrix to the respective parametrized ROM matrices such that they are positive definite.

The first γ -selection method, called *fixed γ -sequence*, is summarized in Algorithm 1. The fixed γ -sequence approach requires a predefined strictly monotonically decreasing sequence $(\gamma_j)_{j \in \mathbb{N}} \subset \mathbb{R}^+$ to define the optimization problem to be solved in each iteration. If the minimum of L for a given γ_j is zero, then for all $s_i \in S$, we have that $\|G(s_i) - G_r(s_i, \theta_j)\|_2 \leq \gamma_j$. Therefore, we terminate the

Algorithm 1: Fixed γ -sequence

Input : FOM transfer function $G \in \mathcal{H}_\infty^{n_u \times n_u}$, initial parametrized ROM transfer function $G_r(\cdot, \theta_0) \in \mathcal{RH}_\infty^{n_u \times n_u}$ with parameter $\theta_0 \in \mathbb{R}^{n_\theta}$, sample point set $S \subset i\mathbb{R}$, strictly monotonically decreasing sequence $(\gamma_j)_{j \in \mathbb{N}} \subset \mathbb{R}^+$, termination tolerance $\varepsilon > 0$

Output: optimal ROM parameters $\theta_{\text{opt}} \in \mathbb{R}^{n_\theta}$

```
1 for  $j = 0, 1, 2, 3, \dots$  do
2   | Solve the minimization problem  $\alpha_{j+1} := \min_{\theta \in \mathbb{R}^{n_\theta}} L(\gamma_{j+1}, G, G_r(\cdot, \theta), S)$  with minimizer
      |  $\theta_{j+1} \in \mathbb{R}^{n_\theta}$ , initialized at  $\theta_j$ .
3   | if  $\alpha_{j+1} > \varepsilon$  then
4     |   | Set  $\theta_{\text{opt}} := \theta_j$ .
5     |   | Break.
6   | end
7 end
```

inner optimization loop (in line 2 of Alg. 1), when the value of L is less than a prescribed *termination tolerance* ε . In this case, the optimization is started again for the smaller value γ_{j+1} . If there is at least one value $s_i \in S$, for which $\|G(s_i) - G_r(s_i, \theta_j)\|_2 > \gamma_j + \varepsilon$ after the optimization (which is then not terminated by falling below the termination tolerance but either by converging to a local optimum or exceeding the number of permitted optimization steps), then the algorithm is terminated. In the numerical experiments reported in Section 5, we have used Alg. 1 with termination tolerance $\varepsilon = 10^{-14}$.

Another approach to select subsequent values for γ is based on bisection and outlined in Algorithm 2. The difference to the previous γ -selection approach is that here, the user only needs to provide an upper bound γ_u and then γ is adjusted based on the results of the optimization of the ROM parameters. In our experiments this takes longer than Algorithm 1 and leads to slightly larger \mathcal{H}_∞ errors.

Algorithm 2: γ -Bisection

Input : FOM transfer function $G \in \mathcal{H}_\infty^{n_u \times n_u}$, initial ROM transfer function $G_r(\cdot, \theta_0) \in \mathcal{RH}_\infty^{n_u \times n_u}$ with parameter $\theta_0 \in \mathbb{R}^{n_\theta}$, sample point set $S \subset i\mathbb{R}$, upper bound $\gamma_u > 0$, bisection tolerance $\varepsilon_1 > 0$, termination tolerance $\varepsilon_2 > 0$

Output: optimal ROM parameters $\theta_{\text{opt}} \in \mathbb{R}^{n_\theta}$

```
1 Set  $j = 0$  and  $\gamma_l := 0$ .
2 while  $(\gamma_u - \gamma_l)/(\gamma_u + \gamma_l) > \varepsilon_1$  do
3   | Set  $\gamma = (\gamma_u + \gamma_l)/2$ .
4   | Solve the minimization problem  $\alpha_{j+1} := \min_{\theta \in \mathbb{R}^{n_\theta}} L(\gamma, G, G_r(\cdot, \theta), S)$  with minimizer
      |  $\theta_{j+1} \in \mathbb{R}^{n_\theta}$ , initialized at  $\theta_j$ .
5   | if  $\alpha_{j+1} > \varepsilon_2$  then
6     |   | Set  $\gamma_l := \gamma$ .
7   | else
8     |   | Set  $\gamma_u := \gamma$ .
9   | end
10  | Set  $j := j + 1$ .
11 end
12 Set  $\theta_{\text{opt}} := \theta_j$ .
```

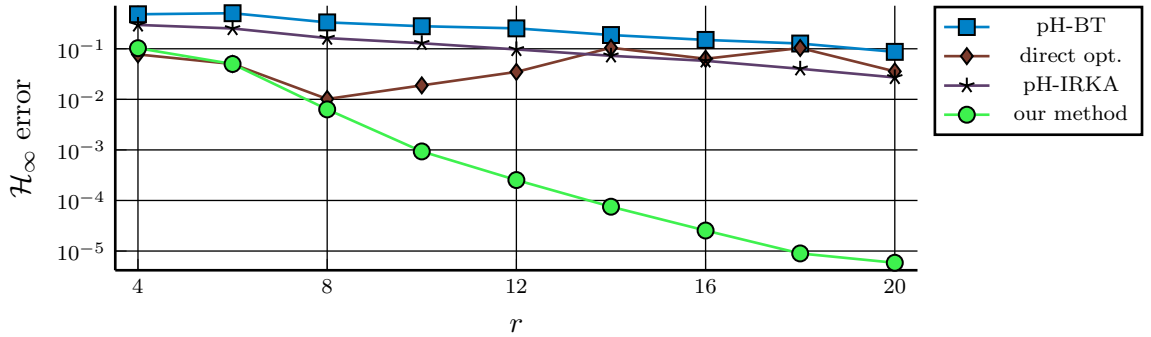


Figure 2: \mathcal{H}_∞ errors for different MOR methods for varying ROM orders. The FOM is the mass-spring-damper pH system in [20] of order 100.

5 Numerical Experiments

In the following, we compare the approximation quality in terms of the \mathcal{H}_∞ norm and the \mathcal{H}_2 norm of our method to other, previously established, methods that also preserve the structure of either a pH or SSO system. For both model types we provide a comparison of our method with the structure preserving MOR methods presented in Section 2. For both model structures our method outperforms the other methods by a few orders of magnitude with respect to accuracy in terms of the \mathcal{H}_∞ norm.

5.1 Port-Hamiltonian Systems

The pH model we consider is used in [20] to showcase the effectiveness of a structure preserving adaption of IRKA. It models again a mass-spring-damper system. The inputs are two forces applied to the first two masses and the outputs are their respective velocities. For details on the setup of the system matrices we refer to [20]. In our experiments, we follow [20] and first use a FOM with the moderate state dimension of 100 in order to deliver a thorough analysis of the error based on \mathcal{H}_∞ and \mathcal{H}_2 norms. For the sampling points, we compute 800 logarithmically spaced points between 10^{-5} and 10^3 . We add a few sampling points outside of this interval, namely $0, 10^{-8}, 10^{-7}, 10^{-6}, 10^4, 10^5$, and 10^6 , to also accurately collect information on the asymptotic behavior of the original model. We discuss different implementation variants of our method in Section 4. The results shown here are obtained with Algorithm 1, in which the objective function L is minimized for a sequence of monotonically decreasing $(\gamma_j)_{j \in \mathbb{N}}$ until the computed minimum is different from 0. Here we choose $(\gamma_j)_{j \in \mathbb{N}} = (1, 0.5, 0.2, 0.1, 0.05, 0.02, 0.01, \dots)$.

In Figure 2, we show the \mathcal{H}_∞ norm of the difference between the original transfer function and the transfer function of the ROM computed with different pH structure preserving MOR methods. It is important to note that both parameter optimization approaches (direct opt. and our method) yield a higher accuracy for small values of r . However the direct \mathcal{H}_∞ optimization leads to worse approximations as r increases. On the other hand, using our objective function, the \mathcal{H}_∞ error continues to decrease for larger r . Finally, our approximation outperforms all other structure preserving methods by more than three orders of magnitude for this benchmark system.

In Figure 3, the maximum singular values of the transfer function of the error between the given

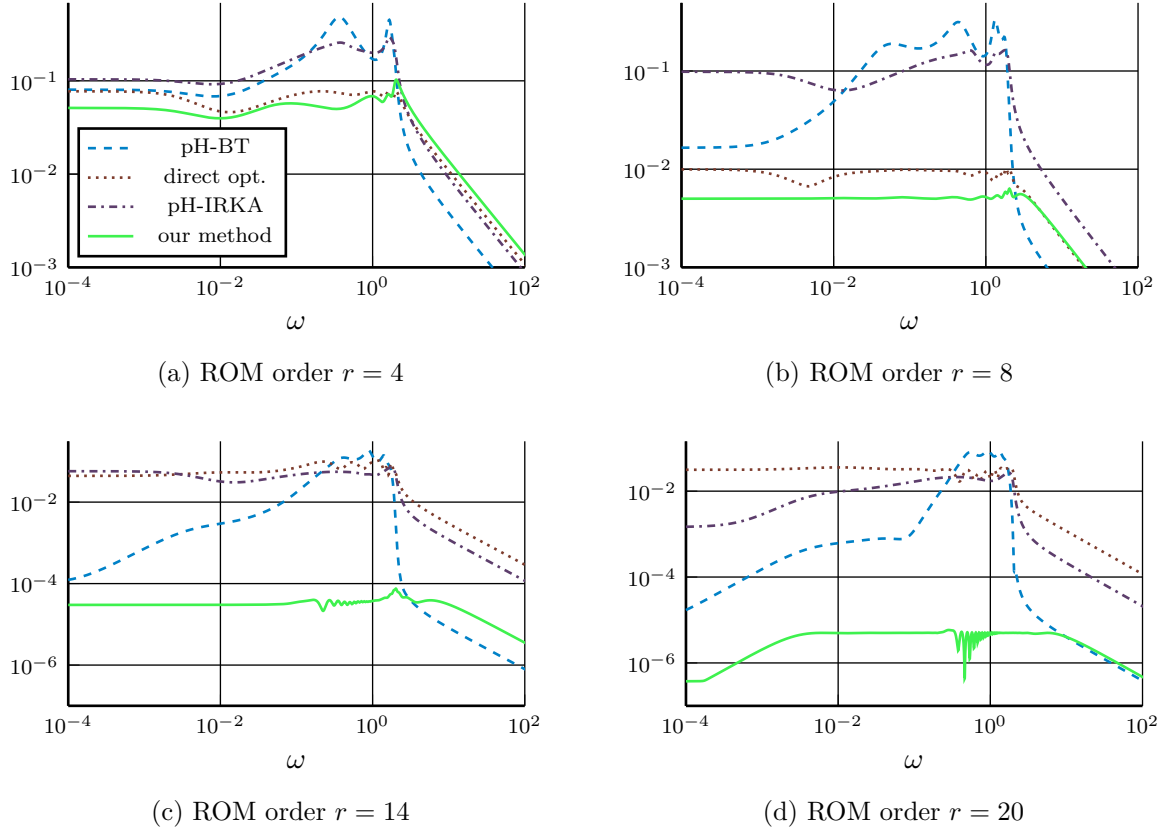


Figure 3: Maximal singular value of the error transfer function for different MOR methods as r is varied. The FOM is the mass-spring-damper pH system in [20] of order 100.

model and its approximations obtained from the different MOR methods are shown for different r . As r increases, the error obtained with our method tends to get less oscillatory in larger parts of the frequency spectrum. This desired behavior is not achieved with the other methods.

Furthermore, it can be observed that the approximation is consistently better for most frequencies such that the larger \mathcal{H}_∞ error which the other methods produce is not just due to a few areas on the imaginary axis where the transfer function is approximated poorly. Therefore, even though our method tends to minimize the \mathcal{H}_∞ error, in the comparison of the \mathcal{H}_2 errors in Figure 4 the approximation error is again several orders of magnitude smaller when using our method.

In order to illustrate the performance of our method also in large-scale settings, for the next experiments we use the FOM dimension $n = 20\,000$. In Figure 5, we compare the performance of our method against pH-IRKA, since both methods rely only on sparse linear solves and are thus appropriate for the large-scale case. With our method, we again obtain an error that is lower by a few orders of magnitude. In fact, in [20], it is reported that the \mathcal{H}_∞ error when using pH-IRKA is still above 10^{-4} for ROMs of order 50.

In our experiments, the runtime of our algorithm is mainly driven by the choice of the ROM order. In our numerical study for the pH system of order 100, the algorithm terminated after 28.76s for a ROM order of 4, while it took 5214.43s to terminate for the maximal ROM order of 20. This

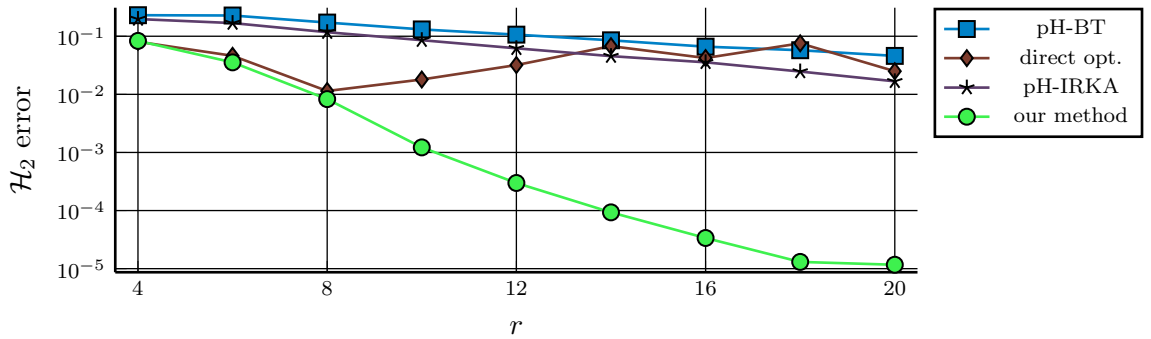


Figure 4: \mathcal{H}_2 error for different MOR methods as ROM order r is varied. The FOM is the mass-spring-damper pH model in [20] of order 100.

Table 1: Number of iterations in the optimization step in (Alg. 1, line 2) as γ is reduced. The FOM is the pH system of order 100.

r	γ_6	γ_7	γ_8	γ_9	γ_{10}	γ_{11}	γ_{12}	γ_{13}	γ_{14}	γ_{15}	γ_{16}	γ_{17}	γ_{18}	γ_{19}
4	23	35	83	—	—	—	—	—	—	—	—	—	—	—
6	1	10	13	40	—	—	—	—	—	—	—	—	—	—
8	0	10	18	22	30	34	37	—	—	—	—	—	—	—
10	0	10	23	25	29	36	40	44	49	58	75	—	—	—
12	0	2	21	32	36	36	45	55	53	50	65	76	100	198

is mostly due to the more expensive gradient computation and increased number of iterations for the larger ROMs. On the other hand, the FOM only has to be sampled once in the beginning. Thus the FOM order does not have a major influence on the runtime in our experiments. However, note that in some situations the sampling procedure may also be expensive. This is especially the case if iterative linear system solvers such as GMRES have to be used. If there are no good preconditioners available, then the solution of the involved linear systems can be expensive due to the large number of iterations until convergence.

Since pH-IRKA converged in well under a minute in each experiment, our method is not yet competitive with respect to runtime. However, since MOR is usually performed offline to speed up simulations or the computation of a control signal, we believe that the extremely increased accuracy well compensates for the increased runtime. Furthermore, our implementation is not yet optimized for speed. Note that as γ is reduced during the course of our method, the number of iterations during the gradient based optimization increases. This behavior can be observed in Table 1. This usually makes the final reduction steps the most expensive ones. To alleviate this problem, one can prescribe a desired level of accuracy. Then our algorithm can be modified to work for a fixed value of γ . If the desired accuracy level γ can be achieved, then this will be much faster than using our algorithm for a sequence of γ -values. In particular, since larger values of γ lead to fewer iterations (cf. Table 1), we can trade off a lower accuracy of the ROM for a faster termination of our MOR method.

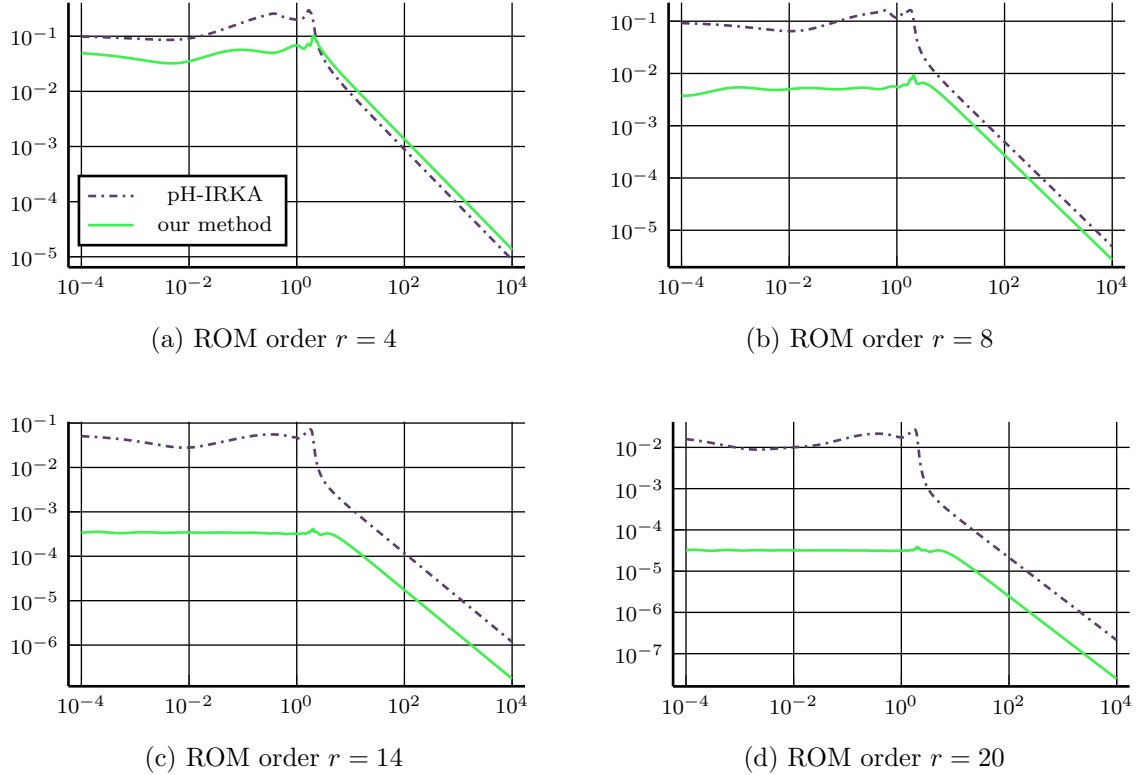


Figure 5: Maximal singular value of the error transfer function for different MOR methods as r is varied. The FOM is the mass-spring-damper pH system in [20] of order 20 000.

5.2 Second Order Systems

The scalable mechanical system that we use to showcase the efficiency of our method for second order systems is introduced in [45] as triple mass-spring-damper chain. We refer to [45] for a detailed description of the mass-spring-damper chain model as well as the setup of the system matrices M , D , and K . In order to compare our method with second order balanced truncation and to compute the \mathcal{H}_∞ norm using [9] for a globally valid result, we choose the state dimension $n_x = 301$ for our experiments. Since in [45], no input or output mapping is provided, we set $B := [I_3 \ 0_{n_x-3 \times 3}]^\top$, which corresponds to actuation and measurement at the first three masses. For the sampling points we choose 300 logarithmically spaced points between 10^{-4} and 10^3 . Again, we add a few points outside of this interval, namely $0, 10^{-8}, 10^{-7}, 10^{-6}, 10^{-4}, 10^4, 10^5$, and 10^6 . The γ sequence was chosen as in the previously described experiments.

In Figure 6, we compare the \mathcal{H}_∞ norm of the error transfer functions for ROMs with varying order. Note that our proposed method outperforms the other methods for structure preserving model order reduction for all tested values of r by a huge margin. To obtain a ROM with an \mathcal{H}_∞ error of less than 10^{-6} , using our method, a reduced model order of only 11 is needed, while the other methods only reach this accuracy with a reduced model order of 21. However, it is interesting to note that beyond a reduced model order of $r = 15$, the \mathcal{H}_∞ error does not further decrease significantly when our method is employed. We believe that this could be an effect of numerical

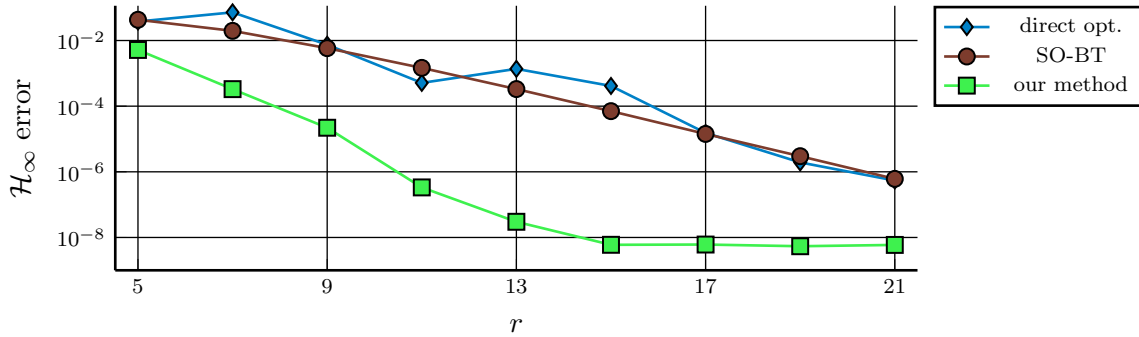


Figure 6: \mathcal{H}_∞ errors for different MOR methods as ROM order r is varied. The FOM is the second order mechanical system with $n_x = 301$.

errors that may have a stronger influence on the result for very small values of γ . Moreover, since the optimization problem in line 4 of Alg. 1 is nonconvex, it may have only converged to a local but not a global minimizer.

Looking at the error transfer functions for different reduced orders which are depicted in Figure 7 it can be observed that the error using our method is nearly constant over a wide frequency range. The other methods lead to an error that is larger for almost all frequencies but also more oscillatory. Using our method, the error gets less oscillatory for a larger reduced order, while the spikiness increases when the direct optimization approach is used. We assume that this is due to the fact that the gradient of the \mathcal{H}_∞ norm of the error does not simultaneously lead to a descend direction that decreases the magnitude of all peaks when using the direct optimization approach since only the largest peak is considered in the gradient. On the other hand, minimizing L , we can consider different frequencies at which the error is large at once and in this way find a better descend direction.

6 Conclusions and Outlook

In this paper, we have developed a new approach to MOR based on direct optimization of the structured ROM's state space realization. Instead of directly minimizing the \mathcal{H}_∞ or \mathcal{H}_2 error, we have proposed to iteratively apply a leveled least squares objective function. This reveals a globally better behavior. We have demonstrated the benefits of our method and its superior performance compared to other structure preserving MOR methods in a couple of numerical experiments.

The method is applicable in a far broader setting that we plan to explore in subsequent works. In the following we summarize two future research directions.

- Until now, we have chosen logarithmically spaced sample points on the imaginary axis. However, we may decrease the computational footprint and necessary a priori knowledge about the critical intervals of the FOM by adaptive sampling.
- We plan to explore the utilization of this method in parametric MOR in which the FOM depends on several parameters and the ROM should mimic the behavior of the FOM for all admissible parameter settings.

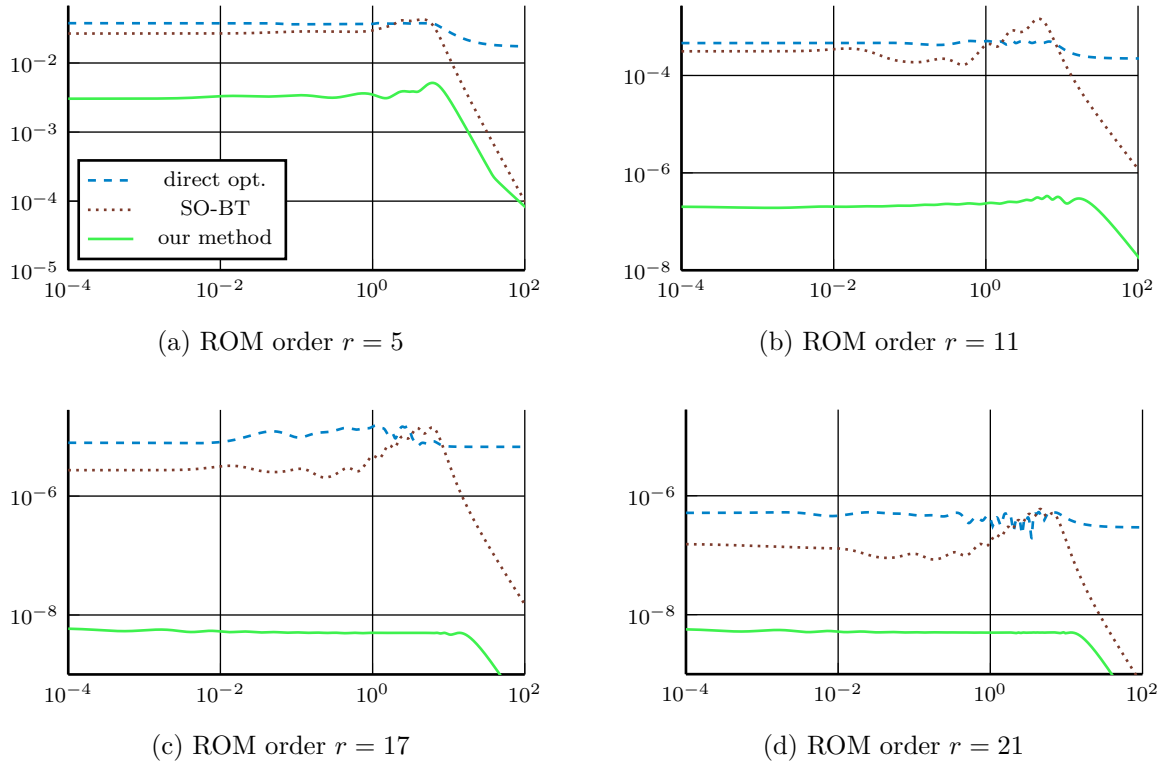


Figure 7: Maximum singular values of the error transfer function between the FOM (second order mechanical system with dimension $n_x = 301$) for different structure preserving MOR methods as r is varied.

Acknowledgement

We thank Volker Mehrmann (TU Berlin) for his useful comments on an earlier version of this manuscript.

References

- [1] N. Aliyev, P. Benner, E. Mengi, P. Schwerdtner, and M. Voigt. Large-scale computation of \mathcal{L}_∞ -norms by a greedy subspace method. *SIAM J. Matrix Anal. Appl.*, 38(4):1496–1516, 2017.
- [2] A. C. Antoulas. *Approximation of Large-Scale Dynamical Systems*, volume 6 of *Adv. Des. Control*. SIAM Publications, Philadelphia, PA, 2005.
- [3] A. C. Antoulas, C. A. Beattie, and S. Gürgencin. *Interpolatory Methods for Model Reduction*. SIAM Publishing, Philadelphia, PA, 2020.
- [4] Z. Bai and Y.-F. Su. Dimension reduction of large-scale second-order dynamical systems via a second-order Arnoldi method. *SIAM J. Sci. Comput.*, 26(5):1692–1709, 2005.

- [5] C. Beattie and P. Benner. \mathcal{H}_2 -optimality conditions for structured dynamical systems. Preprint MPIMD14-18, Max Planck Institute Magdeburg, 2014.
- [6] C. Beattie, V. Mehrmann, and H. Xu. Port-Hamiltonian realizations of linear time invariant systems. Preprint 23-2015, Institute of Mathematics, Technische Universität Berlin, 2015.
- [7] R. S. Beddig, P. Benner, I. Dorschky, T. Reis, P. Schwerdtner, M. Voigt, and S. W.R. Werner. Model reduction for second-order dynamical systems revisited. *PAMM Proc. Appl. Math. Mech.*, 19(1):e201900224, 2019.
- [8] P. Benner, P. Kürschner, and J. Saak. An improved numerical method for balanced truncation for symmetric second order systems. *Math. Comput. Model. Dyn. Syst.*, 19(6):593–615, 2013.
- [9] S. Boyd and V. Balakrishnan. A regularity result for the singular values of a transfer matrix and a quadratically convergent algorithm for computing its \mathbf{L}_∞ -norm. *Systems Control Lett.*, 15(1):1–7, 1990.
- [10] N. A. Bruinsma and M. Steinbuch. A fast algorithm to compute the H_∞ -norm of a transfer function matrix. *Systems Control Lett.*, 14(4):287–293, 1990.
- [11] A. Bunse-Gerstner, D. Kubalińska, G. Vossen, and D. Wilczek. h_2 -norm optimal model reduction for large scale discrete dynamical MIMO systems. *J. Comput. Appl. Math.*, 233(5):1202–1216, 2010.
- [12] J. V. Burke, A. S. Lewis, and M. L. Overton. A robust gradient sampling algorithm for nonsmooth, nonconvex optimization. *SIAM J. Optim.*, 15(3):751–779, 2005.
- [13] Y. Chahlaoui, D. Lemonnier, A. Vandendorpe, and P. Van Dooren. Second-order balanced truncation. *Linear Algebra Appl.*, 415(2–3):373–384, 2006.
- [14] F. E. Curtis, T. Mitchell, and M. L. Overton. A BFGS-SQP method for nonsmooth, nonconvex, constrained optimization and its evaluation using relative minimization profiles. *Optim. Methods Softw.*, 32(1):148–181, 2017.
- [15] F. E. Curtis and M. L. Overton. A sequential quadratic programming algorithm for nonconvex, nonsmooth constrained optimization. *SIAM J. Optim.*, 22(2):474–500, 2012.
- [16] F. M. Dopico, P. W. Lawrence, J. Pérez, and P. Van Dooren. Block Kronecker linearizations of matrix polynomials and their backward errors. *Numer. Math.*, 140(2):373–426, 2018.
- [17] I. Dorschky, T. Reis, and M. Voigt. Balanced truncation model reduction for symmetric second order systems – A passivity-based approach. Preprint arXiv:2006.09170, 2020.
- [18] M. A. Freitag, A. Spence, and P. Van Dooren. Calculating the H_∞ -norm using the implicit determinant method. *SIAM J. Matrix Anal. Appl.*, 35(2):619–635, 2014.
- [19] S. Gugercin, A. C. Antoulas, and C. Beattie. \mathcal{H}_2 model reduction for large-scale linear dynamical systems. *SIAM J. Matrix Anal. Appl.*, 30(2):609–638, 2008.
- [20] S. Gugercin, R. V. Polyuga, C. Beattie, and A. van der Schaft. Structure-preserving tangential interpolation for model reduction of port-Hamiltonian systems. *Automatica J. IFAC*, 48(9):1963–1974, 2012.

- [21] N. Guglielmi, M. Gürbüzbalaban, and M. L. Overton. Fast approximation of the H_∞ -norm via optimization over spectral value sets. *SIAM J. Matrix Anal. Appl.*, 34(2):709–737, 2013.
- [22] C. Guiver and M. R. Opmeer. Error bounds in the gap metric for dissipative balanced approximations. *Linear Algebra Appl.*, 439(12):3659–3698, 2013.
- [23] C. Hartmann, V.-M. Vulcanov, and C. Schütte. Balanced truncation of linear second-order systems: a Hamiltonian approach. *Multiscale Model. Simul.*, 8(4):1348–1367, 2010.
- [24] S.-A. Hauschild, N. Marheineke, and V. Mehrmann. Model reduction techniques for linear constant coefficient port-Hamiltonian differential-algebraic systems. *Control Cybernet.*, 48(1):125–152, 2019.
- [25] R. Ionutiu, J. Rommes, and A. C. Antoulas. Passivity-preserving model reduction using dominant spectral zero interpolation. *IEEE Trans. Computer-Aided Design*, 27(12):2250–2263, 2008.
- [26] P. Lancaster. On eigenvalues of matrices dependent on a parameter. *Numer. Math.*, 6:377–387, 1964.
- [27] V. Mehrmann and P. Van Dooren. Structured backward errors for eigenvalues of linear port-Hamiltonian descriptor systems. *SIAM J. Matrix Anal. Appl.*, 2020. Accepted for publication, also available as Preprint arXiv:2005.04744.
- [28] V. Mehrmann and T. Stykel. Balanced truncation model reduction for large-scale systems in descriptor form. In P. Benner, V. Mehrmann, and D. Sorensen, editors, *Dimension Reduction of Large-Scale Systems*, volume 45 of *Lect. Notes Comput. Sci. Eng.*, chapter 3, pages 89–116. Springer, Berlin, 2005.
- [29] D. G. Meyer and S. Srinivasan. Balancing and model reduction for second-order form linear systems. *IEEE Trans. Automat. Control*, 41(11):1632–1644, 1996.
- [30] P. K. Mogensen and A. N. Riseth. Optim: A mathematical optimization package for Julia. *J. Open Source Softw.*, 3(24):615–618, 2018.
- [31] R. Ober. Balanced parametrization of classes of linear systems. *SIAM J. Control Optim.*, 29(6):1251–1287, 1991.
- [32] H. K. F. Panzer, T. Wolf, and B. Lohmann. H_2 and H_∞ error bounds for model order reduction of second order systems by Krylov subspace methods. In *Proceedings of the 2013 European Control Conference*, pages 4484–4489, Zürich, Switzerland, 2013.
- [33] I. R. Petersen and A. Lanzon. Feedback control of negative imaginary systems. *IEEE Control Syst. Mag.*, 30(5):54–72.
- [34] R. V. Polyuga. *Model Reduction of Port-Hamiltonian Systems*. Proefschrift, University of Groningen, 2010.
- [35] R. V. Polyuga and A. J. van der Schaft. Structure preserving model reduction of port-Hamiltonian systems. In *Proceedings of the 18th International Symposium on Mathematical Theory of Networks and Systems*, Blacksburg, VA, 2008.
- [36] T. Reis and T. Stykel. Balanced truncation model reduction of second-order systems. *Math. Comput. Model. Dyn. Syst.*, 14(5):391–406, 2008.

- [37] J. Rommes and N. Martins. Computing transfer function dominant poles of large-scale second-order dynamical systems. *IEEE Trans. Power Syst.*, 21(4):1471–1483, 2006.
- [38] A. Ruszczyński. *Nonlinear Optimization*. Princeton University Press, Princeton, NJ, 2006.
- [39] J. Saak, D. Siebelts, and S. W. R. Werner. A comparison of second-order model order reduction methods for an artificial fishtail. *at – Automatisierungstechnik*, 67(8):648–667, 2019.
- [40] B. Salimbahrami. *Structure Preserving Order Reduction of Large Scale Second Order Models*. Dissertation, Fakultät für Maschinenwesen, Technische Universität München, 2005.
- [41] B. Salimbahrami and B. Lohmann. Order reduction of large scale second-order systems using Krylov subspace methods. *Linear Algebra Appl.*, 415(2–3):385–405, 2006.
- [42] P. Schwerdtner, E. Mengi, and M. Voigt. Certifying global optimality for the \mathcal{L}_∞ -norm computation of large-scale descriptor systems, February 2020. Presented at the 21st IFAC World Congress, Berlin, Germany, 2020.
- [43] P. Schwerdtner and M. Voigt. Computation of the \mathcal{L}_∞ -norm using rational interpolation. *IFAC-PapersOnLine*, 51(25):84–89, 2018. 9th IFAC Symposium on Robust Control Design 2018, Florianópolis, Brazil.
- [44] D. C. Sorensen. Passivity preserving model reduction via interpolation of spectral zeros. *Systems Control Lett.*, 54(4):347–360, 2005.
- [45] N. Truhar and K. Veselić. An efficient method for estimating the optimal dampers' viscosity for linear vibrating systems using Lyapunov equation. *SIAM J. Matrix Anal. Appl.*, 31(1):18–39, 2009.
- [46] A. van der Schaft and D. Jeltsema. Port-Hamiltonian systems theory: An introductory overview. *Found. Trends Systems Control*, 1(2–3):173–378, 2014.
- [47] P. Van Dooren, K. A. Gallivan, and P.-A. Absil. \mathcal{H}_2 -optimal model reduction of MIMO systems. *Appl. Math. Lett.*, 21(12):1267–1273, 2008.
- [48] M. Voigt. *On Linear-Quadratic Optimal Control and Robustness of Differential-Algebraic Systems*. Logos, Berlin, 2015. Also as Dissertation, Fakultät für Mathematik, Otto-von-Guericke-Universität Magdeburg, 2015.
- [49] T. Wolf, B. Lohmann, R. Eid, and P. Kotyczka. Passivity and structure preserving order reduction of linear port-Hamiltonian systems using Krylov subspaces. *Eur. J. Control*, 16(4):401–406, 2010.